

Homogeneous Estimation of Moment Magnitude for Small-to-Moderate Magnitude Earthquakes Located near the Border between Japan and Taiwan

by **Tadahiro Kishida, Robert B. Darragh, Yousef Bozorgnia, Chun-Hsiang Kuo, and Hongjun Si**

ABSTRACT

A homogeneous estimate of moment magnitude (M) for small-to-moderate-magnitude (SMM) earthquakes is important to assess regional ground-motion attenuation and seismic hazard. Multiple estimates of M for SMM events are often available from regional agencies. These estimates are typically biased compared with the estimates from a global agency due to limited geographic or azimuthal convergence. The M of SMM earthquakes near the border between Japan and Taiwan is available from both the Broadband Array in Taiwan for Seismology and the Full Range Seismograph Network of Japan for $M > 3$. The M provided by these agencies is compared with that by the Global Centroid Moment Tensor for $M > 4.5$ to estimate the bias and standard deviation of the values. An optimum data fusion of these M s is presented to obtain a homogeneous estimation of M for SMM earthquakes ($4.5 < M < 5.0$) near the border between Japan and Taiwan.

Electronic Supplement: Table of moment magnitudes analyzed in the main article.

INTRODUCTION

The region near the border between Japan and Taiwan is seismologically active. A subduction zone exists along the Ryukyu trench, where the Philippine Sea plate subducts beneath the Eurasian plate. Many large-magnitude earthquakes have occurred in this region historically. For example, an earthquake occurred near Ishigaki Island on 24 April 1771 and produced a tsunami with a run-up height of 30 m on Yaeyama (Nakamura, 2009). Several studies (e.g., Hsu *et al.*, 2012) have also warned of the potential for large earthquakes in this region in the future. Therefore, an assessment of ground-motion models (GMMs) and seismic hazard is critical for this region, and a

consistent (homogeneous) estimate of moment magnitude (M) is essential for the success of these studies.

A homogeneous M catalog is an important parameter used in assessing and applying regional seismic hazard and ground motion compared with global models. Atkinson and McCartney (2005) noted the importance of a homogeneous magnitude scale for small-to-moderate-magnitude (SMM) events to produce an unbiased magnitude recurrence relation for seismic hazard analysis in southwestern British Columbia. Scherbaum *et al.* (2004) documented various magnitude estimates for the St Dié 2003 Earthquake in France and described that a difficulty in applying a global GMM to regional SMM data was the estimation of M because the ground-motion attenuations from the global GMM varied extensively depending on the magnitude type and reporting agency. The Global Centroid Moment Tensor (CMT) is frequently used as the reference M to develop an event catalog (Dziewonski *et al.*, 1981; Ekström *et al.*, 2012). However, the Global CMT mainly provides CMT solutions for events with $M > 5$. Therefore, the M from the regional agencies is used to develop the event catalog when SMM events ($3 < M < 5$) are of interest.

Several studies (e.g., Dreger and Helmberger, 1993; Bernardi *et al.*, 2004) used regional waveform data in analyzing the CMT for local events. The M is generally smaller when determined from regional networks than from global networks given several factors, including long-period response in local network instrumentation, limited azimuthal coverage, and rupture dimensions exceeding the network size (Thio and Kanamori, 1995; Papazachos *et al.*, 1997; Chen *et al.*, 2008; Gasperini *et al.*, 2012; Konstantinou, 2015). Therefore, comparing the M between the regional and global agencies is crucial, and any bias should be corrected to obtain a homogeneous M when using estimates from regional catalogs of M .

Uncertainties in M are also important to use in the development of robust GMMs. Several studies discussed the

development of GMMs that account for the uncertainties in predictor variables (e.g., Rhoades, 1997; Abrahamson and Silva, 2007; Gehl *et al.*, 2011; Stafford, 2014). Recently, Kuehn and Abrahamson (2018) showed that accounting for the uncertainties in \mathbf{M} and time-averaged shear-wave velocity in the upper 30 m reduced both the between-event standard deviation and the within-event/within-station standard deviation by 1%–13%. Therefore, reducing and quantifying the uncertainties in \mathbf{M} is an important step in catalog and database development.

In Japan, the National Research Institute for Earth Science and Disaster Resilience started installing a broadband network in 1994 and has been routinely providing CMT solutions since 1997 through the Full Range Seismograph Network of Japan (F-net; Fukuyama *et al.*, 1998). Similarly, the Japan Meteorological Agency has provided CMT solutions since 1994 using data from their broadband network. Only the estimates of \mathbf{M} from F-net are analyzed in the present study because of data availability and coverage of the study area. The minimum \mathbf{M} for this network is ~ 3.4 .

In Taiwan, the Broadband Array in Taiwan for Seismology (BATS) has been providing CMT solutions routinely since 1995, following the methodology developed by the Institute of Earth Sciences (IES) in 1992 (Kao *et al.*, 1998). In addition, the Central Weather Bureau in Taiwan has been offering CMT solutions since 2005 by adopting a similar methodology. A monitoring system for real-time moment tensor (MT) has been operational in Taiwan since 2010 for earthquakes with $\mathbf{M} > 3$ (Lee *et al.*, 2014). Only the \mathbf{M} from BATS is analyzed in this study because of data availability and the computation methodology. The minimum \mathbf{M} from this network is ~ 3.2 .

The present study uses the \mathbf{M} estimated by two regional agencies, namely, F-net in Japan and BATS in Taiwan, for earthquakes with $\mathbf{M} > 3.2$ near the border between these countries to estimate a homogenous \mathbf{M} for inclusion in the catalog. These \mathbf{M} s are compared with those from the Global CMT when available. The bias and standard deviation in \mathbf{M} are calculated for each agency on the basis of the comparison. A multivariate methodology is presented to obtain an optimum linear combination of these estimates of \mathbf{M} to develop a homogeneous \mathbf{M} estimate for the earthquakes in the catalog in this region.

COMPARISONS OF \mathbf{M} FROM DIFFERENT AGENCIES

The estimates of \mathbf{M} from F-net and BATS are compared against those from the Global CMT for earthquakes near the border between Japan and Taiwan. Table S1 (available in the electronic supplement to this article) presents the event catalog utilized in this study. There are 2570 events in the catalog. The catalog was developed from the International Seismological Centre (ISC) (see Data and Resources). The events were selected from the latitude of 21° – 26° N, and longitude of 120° – 126° E, for the years between 1996 and 2016 (Fig. 1). The seismic moments (M_0) by F-net and BATS (IES, 1996) are obtained from their websites (see Data and Resources), in which the catalog includes events from 2000 to 2016 for F-net

and from 1996 to 2016 for BATS, with \mathbf{M} ranging from 3.2 to 7.1. The M_0 from the Global CMT is obtained from its website (see Data and Resources). The catalogs by Chen and Tsai (2008), Chen *et al.* (2008), and Chang *et al.* (2016) were also reviewed for comparison and quality-assurance checks. Hypocentral locations are selected by giving higher priorities for relocated or reviewed results, such as the Engdahl–van der Hilst–Buland (Engdahl *et al.*, 1998; Engdahl, 2006), ISC, and the National Earthquake Information Center. Figure 1 shows epicentral locations of the analyzed events. The figure also shows the boundaries of the four regions. The boundary lines (north–south and east–west) nearly follow the edges of the Ryuku and Philippine trenches. Figure 1 and Table S1 display the available estimates of \mathbf{M} from the three agencies that vary depending on earthquake magnitude and agency.

The reported M_0 is converted to \mathbf{M} using the following equation:

$$\mathbf{M} = \frac{2}{3} \log_{10}(M_0) - 10.7 \quad (1)$$

(Hanks and Kanamori, 1979), in which M_0 has a unit of $\text{dyn} \cdot \text{cm}$. The use of \mathbf{M} from the three agencies allows estimating the bias and standard deviation in \mathbf{M} . Figure 2 illustrates the distribution of \mathbf{M} in the dataset from the different agencies. A total of 2570 events have at least one estimate of \mathbf{M} from either the Global CMT, F-net, or BATS. Only 11% of these events have \mathbf{M} determined by the Global CMT, and 56% and 13% of the events have \mathbf{M} determined either from F-net or BATS. The remaining 20% of the events have \mathbf{M} from the F-net and BATS. Therefore, 89% of the events have only an estimate of \mathbf{M} from a regional network. Therefore, a method of optimum data fusion is required from the available estimates of \mathbf{M} to calculate homogeneous \mathbf{M} and its standard deviation. The following section presents the estimation of bias and uncertainty for the different agencies using multivariate statistics.

BIAS AND STANDARD DEVIATION FOR $\Delta\mathbf{M}$

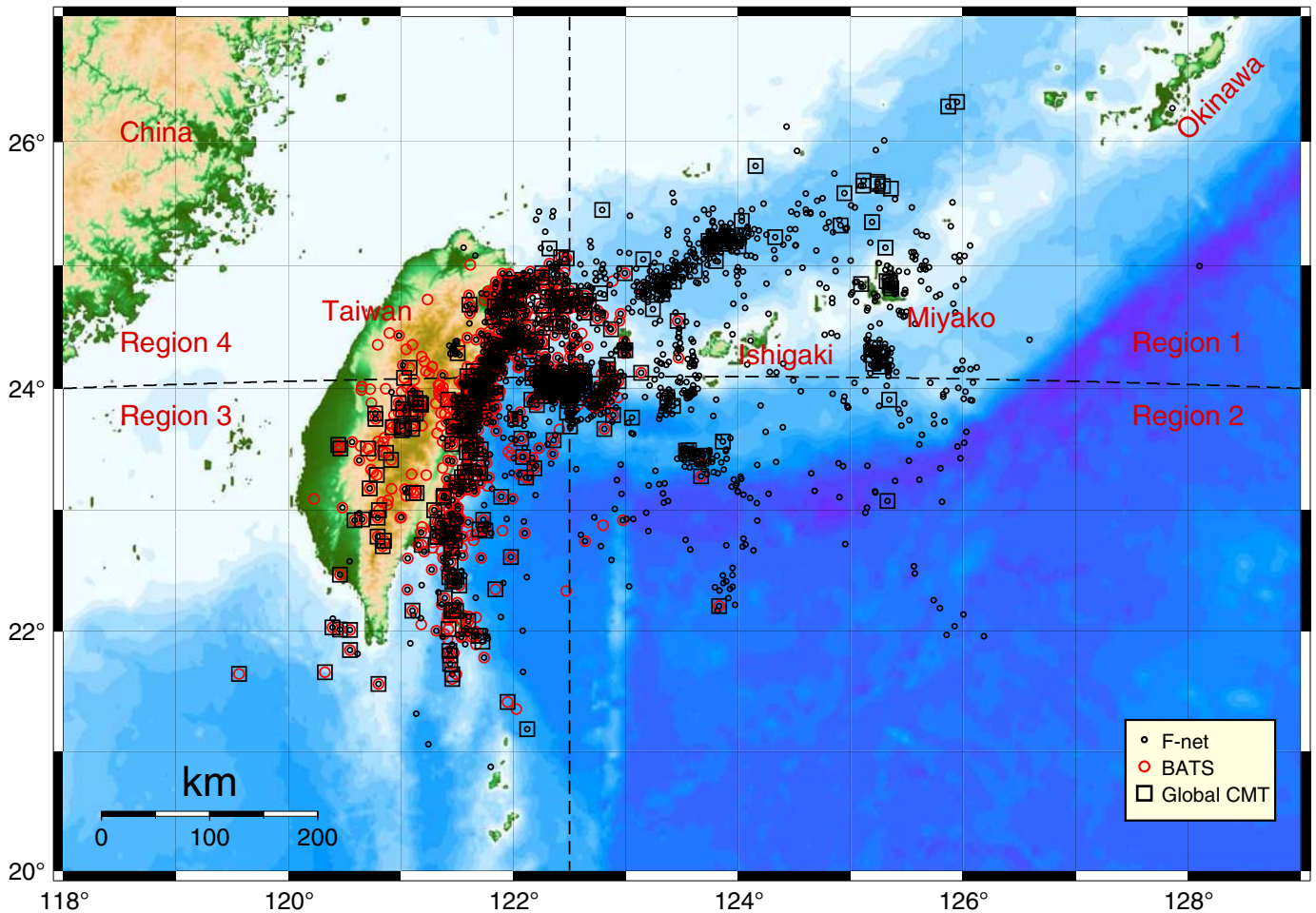
The differences in \mathbf{M} ($\Delta\mathbf{M}$) among the agencies are calculated using the following formulas:

$$\Delta\mathbf{M}_{G-F} = \mathbf{M}_G - \mathbf{M}_F \quad (2)$$

$$\Delta\mathbf{M}_{G-B} = \mathbf{M}_G - \mathbf{M}_B \quad (3)$$

$$\Delta\mathbf{M}_{F-B} = \mathbf{M}_F - \mathbf{M}_B \quad (4)$$

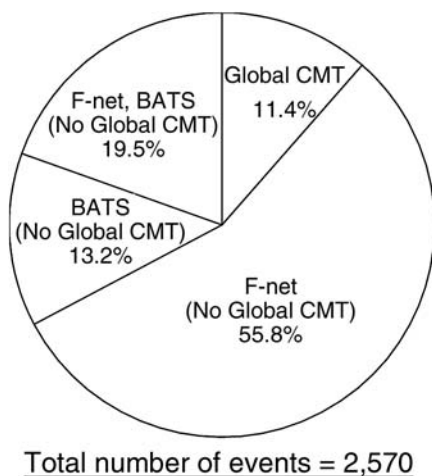
in which subscripts G, F, and B represent Global CMT, F-net, and BATS, respectively. Figure 3a–c demonstrates the variation in $\Delta\mathbf{M}$ among the agencies versus the year. The figures depict the increase in $\Delta\mathbf{M}$ from 2008 to April 2014 between Global CMT and BATS and between F-net and BATS. In contrast, $\Delta\mathbf{M}$ is nearly constant between Global CMT and F-net in Figure 3a. Figure 4a–c illustrates the variation in $\Delta\mathbf{M}$ among



▲ **Figure 1.** Epicenter locations of the analyzed dataset near the border between Japan and Taiwan. The color version of this figure is available only in the electronic edition.

the agencies versus the hypocentral depths for the different regions. The four regions in Figure 4 are shown in Figure 1, and the boundaries are approximately aligned with the trench axes in the region. Because ΔM is approximately constant against

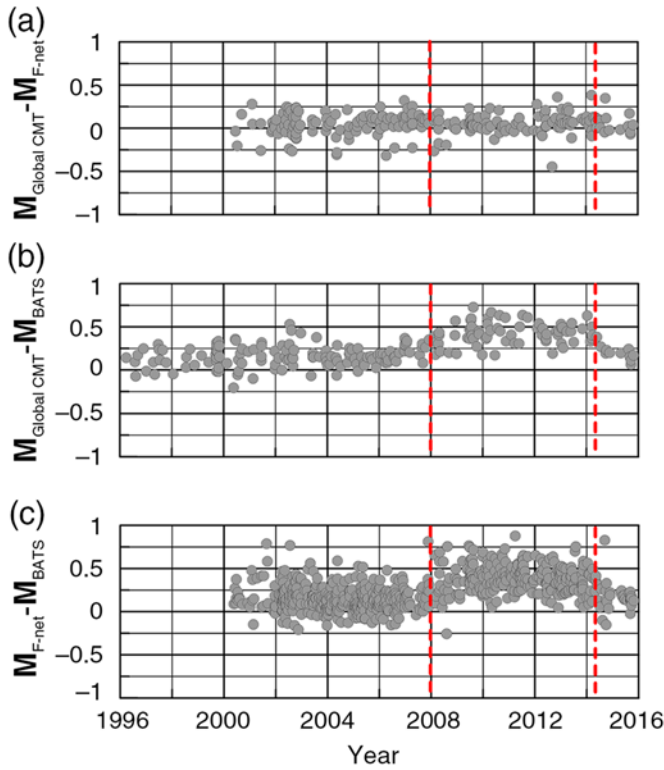
hypocentral depth for various combinations of agencies and regions, no bias was found in the reported M for either depth or the geometry of the reporting network stations, with respect to the trench axes.



▲ **Figure 2.** Distribution of available magnitudes by different agencies in the developed event catalog.

The mean values of ΔM_{G-F} , ΔM_{G-B} , and ΔM_{F-B} were 0.051, 0.166, and 0.154 before 2008 and after April 2014; however, these values were 0.053, 0.430, and 0.388 between 2008 and April 2014. These differences clearly indicate that ΔM_{G-B} and ΔM_{F-B} increased within the time interval from 2008 to April 2014. A t -test for the hypothesis of equal means between the two periods provides $t = 0.107, 15.2,$ and 18.5 for $\Delta M_{G-F}, \Delta M_{G-B},$ and ΔM_{F-B} , correspondingly. These statistics also denote that the mean values of ΔM_{G-B} and ΔM_{F-B} changed during the period 2008 to April 2014. Table 1 summarizes the mean and standard deviation for equations (2)–(4). The average of the values for ΔM_{G-F} is reported in the table given their insignificant difference.

The observation in Table 1 is consistent with the underestimation of M by BATS from 2008 to 2014 considering a technical problem that reduced the waveform amplitude by a factor of 2 during a system upgrade in 2008 (Huang, 2017; W.-T. Liang, personal comm., 2017). F-net and BATS



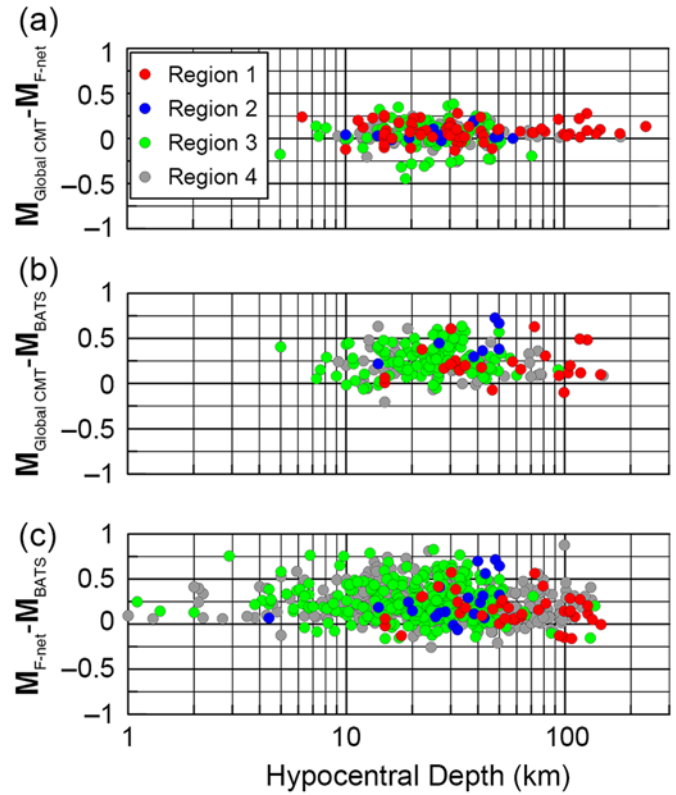
▲ **Figure 3.** Differences in M between agencies versus year. The color version of this figure is available only in the electronic edition.

underpredict M , as determined by the Global CMT, by 0.05 and 0.16–0.43, respectively. Kubo *et al.* (2002) reported the bias of 0.1 for F-net from 1997 to 2000. Similarly, Chen *et al.* (2008) reported a bias of 0.3 for BATS from 1996 to 2005. These reported biases are slightly larger but consistent with the biases obtained in the present study.

UNCERTAINTIES IN M FOR F-NET, BATS, AND GLOBAL CMT

The standard deviation in M (σ_M) for each agency is calculated using the standard deviations in Table 1. If the σ_M for each agency is assumed to be constant and the residuals are independent between two agencies, then σ_M is obtained from the following formula:

$$\sigma_M = \frac{\sigma_{\Delta M}}{\sqrt{2}} \quad (5)$$



▲ **Figure 4.** Differences in M between agencies versus hypocentral depth for different regions for the four regions shown in Figure 1. The color version of this figure is available only in the electronic edition.

(e.g., Kagan, 2002). However, if only the residuals are assumed to be independent among the three agencies, then σ_M can also be computed using the following formulas:

$$\sigma_{M(F)}^2 = \frac{\sigma_{\Delta M(F-G)}^2 + \sigma_{\Delta M(F-B)}^2 - \sigma_{\Delta M(B-G)}^2}{2} \quad (6)$$

$$\sigma_{M(B)}^2 = \frac{\sigma_{\Delta M(B-G)}^2 + \sigma_{\Delta M(F-B)}^2 - \sigma_{\Delta M(F-G)}^2}{2} \quad (7)$$

$$\sigma_{M(G)}^2 = \frac{\sigma_{\Delta M(F-G)}^2 + \sigma_{\Delta M(B-G)}^2 - \sigma_{\Delta M(F-B)}^2}{2} \quad (8)$$

Table 1					
Means and Standard Deviations for Equations (2)–(4)					
	Mean		$\sigma_{\Delta M}$		
	Before 2008 or After April 2014	From 2008 to April 2014	Before 2008 or After April 2014	From 2008 to April 2014	From 2008 to April 2014
ΔM_{G-F}		0.052		0.115	
ΔM_{G-B}	0.166	0.430	0.118		0.129
ΔM_{F-B}	0.154	0.388	0.152		0.168

Table 2
Standard Deviations in \mathbf{M} for Different Agencies and Different Periods by Equations (5)–(8)

Method	Before 2008 or After April 2014			From 2008 to April 2014		
	F-net	BATS	Global CMT	F-net	BATS	Global CMT
Equation (5) with $\Delta\mathbf{M}_{G-F}$	0.081	—	0.081	0.081	—	0.081
Equation (5) with $\Delta\mathbf{M}_{G-B}$	—	0.083	0.083	—	0.091	0.091
Equation (5) with $\Delta\mathbf{M}_{F-B}$	0.107	0.107	—	0.119	0.119	—
Equations (6)–(8)	0.106	0.109	0.045	0.111	0.126	0.029
Mean	0.098	0.100	0.070	0.104	0.112	0.067

BATS, Broadband Array in Taiwan for Seismology; CMT, Centroid Moment Tensor; F-net, Full Range Seismograph Network of Japan.

Equations (6)–(8) do not assume that $\sigma_{\mathbf{M}}$ is constant among the agencies, whereas equation (5) assumes that it is constant between the agencies. Table 2 lists the $\sigma_{\mathbf{M}}$ calculated using equations (5)–(8). The $\sigma_{\mathbf{M}}$ averages for F-net and Global CMT are ~ 0.101 and 0.069 , respectively, and do not show a clear difference over the time interval. In contrast, the $\sigma_{\mathbf{M}}$ average for BATS increases with time from 0.100 to 0.112 by 12% during the period 2008 to April 2014. The $\sigma_{\mathbf{M}}$ for Global CMT has been estimated previously as between 0.07 and 0.08 (Kagan, 2002; Gasperini *et al.*, 2012) on the basis of the comparison of Global CMT and MT catalogs from other agencies; this estimate is consistent with the values in Table 2. Our literature review indicates that the $\sigma_{\mathbf{M}}$ for F-net and BATS has not been reported by any previous study. The results show that the $\sigma_{\mathbf{M}}$ is the smallest for the Global CMT, whereas it is larger for F-net and BATS.

OPTIMAL ESTIMATES FROM AVAILABLE REGIONAL \mathbf{M}

The best estimate of \mathbf{M} is obtained from Table 1 when \mathbf{M} is available from a single agency only, either F-net (\mathbf{M}_F) or BATS (\mathbf{M}_B), as follows.

For F-net

$$\mathbf{M} = \mathbf{M}_F + 0.052 \quad (9)$$

$$\sigma = 0.115. \quad (10)$$

For BATS, before 2008 or after April 2014

$$\mathbf{M} = \mathbf{M}_B + 0.166 \quad (11)$$

$$\sigma = 0.118 \quad (12)$$

from 2008 to April 2014

$$\mathbf{M} = \mathbf{M}_B + 0.430 \quad (13)$$

$$\sigma = 0.129. \quad (14)$$

Equations (9)–(14) can be applied for $\mathbf{M} > 4.5$ because of the \mathbf{M} distribution in \textcircled{E} Table S1.

The optimal weight for these estimates of \mathbf{M} is determined when the \mathbf{M}_F and \mathbf{M}_B estimates are available. The mean and standard deviation of the linear combination of correlated variables are expressed by the following formulas:

$$\boldsymbol{\mu}' = \mathbf{c}\boldsymbol{\mu} \quad (15)$$

$$\sigma'^2 = \mathbf{c}\boldsymbol{\Sigma}\mathbf{c}' \quad (16)$$

(e.g., Johnson and Wichern, 2002), in which $\boldsymbol{\mu}$ and $\boldsymbol{\Sigma}$ are the mean and covariance matrixes of these variables, respectively. \mathbf{c} is a vector of the weights for these variables. $\boldsymbol{\Sigma}$ is expressed by the standard deviation and correlation matrix as follows:

$$\boldsymbol{\Sigma} = \mathbf{V}^{1/2}\boldsymbol{\rho}\mathbf{V}^{1/2}, \quad (17)$$

in which \mathbf{V} and $\boldsymbol{\rho}$ are the diagonal matrixes of the variance and correlation matrix, correspondingly. The following constraint is applied because the weighted average attracts interest:

$$\sum_{i=1}^n c_i = 1. \quad (18)$$

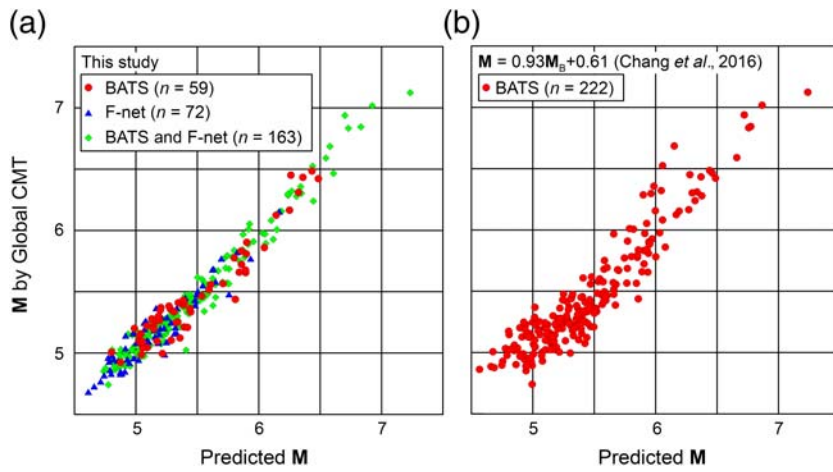
For the bivariate ($N = 2$) case, the following weights of \mathbf{c} are obtained by minimizing the variance in equation (16):

$$c_1 = \frac{\sigma_2^2 - \rho_{12}\sigma_1\sigma_2}{\sigma_1^2 - 2\rho_{12}\sigma_1\sigma_2 + \sigma_2^2} \quad (19)$$

$$c_2 = \frac{\sigma_1^2 - \rho_{12}\sigma_1\sigma_2}{\sigma_1^2 - 2\rho_{12}\sigma_1\sigma_2 + \sigma_2^2}. \quad (20)$$

The weight of c_i when the correlation of ρ_{12} is 0 in equations (19) and (20) is expressed by the inverse-variance-weighted estimates, which are commonly used in past studies to combine the different estimates of \mathbf{M} for event-catalog development

$$c_i = \frac{1/\sigma_i^2}{\sum_{k=1}^n 1/\sigma_k^2} \quad (21)$$



▲ Figure 5. Comparison of the estimated M to the M by Global Centroid Moment Tensor (CMT) (a) combination of Broadband Array in Taiwan for Seismology (BATS) and Full Range Seismograph Network of Japan (F-net), and (b) BATS by [Chang et al. \(2016\)](#). The n represents the number of data points in the analysis. The σ are 0.104 and 0.164 for parts (a) and (b), respectively. The color version of this figure is available only in the electronic edition.

(e.g., [EPRI/DOE/NRC, 2012](#)). The ρ_{12} between the residuals from equations (2) and (3) is obtained as 0.150. c_1 and c_2 are obtained by substituting $\sigma_{\Delta M(G-F)}$ and $\sigma_{\Delta M(G-B)}$ from Table 1 with ρ in equations (19) and (20). These weights are combined with the observed biases, and the M is estimated from M_F and M_B using the following equations:

Before 2008 or after April 2014

$$M = 0.515(M_F + 0.052) + 0.485(M_B + 0.166) \quad (22)$$

$$\sigma = 0.088 \quad (23)$$

from 2008 to April 2014

$$M = 0.567(M_F + 0.052) + 0.433(M_B + 0.430) \quad (24)$$

$$\sigma = 0.092. \quad (25)$$

These equations indicate that the estimate of M for these data is obtained by approximately the arithmetic mean of M from F-net and BATS after correcting for the regional biases compared with that from the Global CMT. This condition occurs only in this case when $\sigma_{\Delta M(G-F)}$ and $\sigma_{\Delta M(G-B)}$ have similar values (Table 1).

Figure 5a,b shows the comparisons of the estimated M from equations (9)–(24) and those estimated by [Chang et al. \(2016\)](#) against M from the Global CMT. The M estimated by [Chang et al. \(2016\)](#) is based on the following regression model:

$$M = 0.93M_B + 0.61. \quad (26)$$

The standard deviation of equation (26) is not presented in [Chang et al. \(2016\)](#). Figure 5a shows that the estimated M in this study reasonably fits the M from the Global CMT with σ of 0.104. This σ is reasonably consistent with the values in equations (10), (12), (14), (23), and (25). Figure 5b also shows that the estimated M by [Chang et al. \(2016\)](#) reasonably fits the M from the Global CMT with σ of 0.164. The smaller standard deviation in this study (Fig. 5a) than [Chang et al. \(2016\)](#) (Fig. 5b) is attributed to the fact that this study uses a different equation (13) from the year 2008 to April 2014 to convert M from BATS to the Global CMT and uses a linear combination of M from BATS and F-net based on multivariate statistics when both estimates are available. These differences resulted in the lower σ in this study than that in [Chang et al. \(2016\)](#).

In summary, this article proposes a methodology for obtaining the optimal M for SMM events when multiple estimates of M are available for earthquakes located near the border between Japan and Taiwan. Similar issues are observed in many regions in the world, such as Iran ([Kishida et al., 2018](#)), but this approach has not been discussed based on our literature review. The presented approach is useful in applications in which multiple estimates of M for SMM events are available from different regional agencies and an estimate from the Global CMT is not available, due to event size.

CONCLUSIONS

The region near the border between Japan and Taiwan is seismologically active. A homogeneous catalog of M for SMM events is an important parameter used in the assessment of regional seismic hazard and to compare regional GMMs with global models. The BATS in Taiwan and F-net in Japan provide estimates of M for many small events with $M > 3$ in this region. These estimates of M from regional agencies were compared with the estimate from the Global CMT to calculate bias and standard deviation. This comparison showed that the M was smaller by 0.052 in F-net than in the Global CMT for the entire dataset from 2000 to 2016. The M was smaller by 0.166 in BATS than in the Global CMT before 2008 or after April 2014, but its bias increased to 0.430 from 2008 to April 2014. The difference in bias for BATS between these time intervals was attributed to an error in the waveform amplitude used by the agency to compute M_0 . This difference occurred due to an error during a system upgrade ([Huang, 2017](#), W.-T. Liang, personal comm., 2017). The $\sigma_{\Delta M}$ between BATS and other agencies also increased by 10% during this period.


The σ_M for the different agencies was calculated using the $\sigma_{\Delta M}$ from the dataset. The uncertainties in M were assumed to be independent among these agencies, using multivariate statistics for the analysis. The analysis indicated that the σ_M from

the Global CMT is the smallest, with a mean value of 0.069. This value is consistent with past studies that found that σ_M ranges from 0.07 to 0.08 for the Global CMT (Kagan, 2002; Gasperini *et al.*, 2012). The σ_M from F-net and BATS was ~ 0.104 , which is larger than the value for the Global CMT. The equations for calculating the uncertainties in \mathbf{M} from the three agencies (i.e., equations 6–8) and the σ_M values for F-net and BATS are presented for the first time in this article.

The best estimate for \mathbf{M} depended on the available \mathbf{M} from F-net and BATS. The estimate of \mathbf{M} for the catalog was obtained by adjusting the bias for each agency from the Global CMT when \mathbf{M} was available from either the F-net or BATS. The optimal estimate of \mathbf{M} was obtained by a weighted average of the \mathbf{M} when \mathbf{M} was available from both F-net and BATS. The weights were determined based on the $\sigma_{\Delta M}$ from F-net or BATS to the Global CMT and with consideration of the correlation among these residuals. This approach was based on multivariate statistics and has not been used previously by other groups to estimate \mathbf{M} for SMM events when multiple estimates of \mathbf{M} were available from regional agencies. The weights showed that the best estimates of \mathbf{M} in this case are approximately obtained by the arithmetic mean of two regional estimates of \mathbf{M} . This result was due to the similarity of $\sigma_{\Delta M}$ between these agencies.

The estimated \mathbf{M} s in this study were compared with those by Chang *et al.* (2016). The results show clear improvements by this study as confirmed by a smaller σ . The lower σ is due to the development of a different equation for the time period from 2008 to April 2014 to convert \mathbf{M} from BATS to the Global CMT that adjusted for a technical problem in the calculation of \mathbf{M} by BATS, and a linear combination of \mathbf{M} by BATS and F-net was used based on multivariate statistics. The approach presented in this article can be applied to any region to obtain an optimum estimate of \mathbf{M} for SMM events when multiple estimates of \mathbf{M} are available from regional agencies (e.g., Kishida *et al.*, 2018).

DATA AND RESOURCES

The event catalog was developed from publicly available data as part of the Pacific Earthquake Engineering Research Center (PEER) Next Generation Attenuation (NGA)-Subduction project. The catalog was developed using hypocentral information from the International Seismological Center (ISC) website (<http://www.isc.ac.uk/iscbulletin/search/catalogue/>, last accessed March 2018) and the studies of Chen and Tsai (2008), Chen *et al.* (2008), and Chang *et al.* (2016). M_0 was obtained from the Full Range Seismograph Network of Japan (F-net; <http://www.fnet.bosai.go.jp/top.php>, last accessed March 2018), the Broadband Array in Taiwan for Seismology (BATS; <http://bats.earth.sinica.edu.tw>, last accessed March 2018), and the Global Centroid Moment Tensor (CMT; <http://www.globalcmt.org/>, last accessed March 2018). The dataset analyzed in this article is provided as an  electronic supplement with the calculated homogenous moment magnitude. The majority of data analyses were conducted using the program R, which is available from <http://www.r-project.org/>

(last accessed August 2017), and many of the figures were prepared using Grapher (<http://www.goldensoftware.com/products/grapher>, last accessed August 2017) and Generic Mapping Tools v.3.4 (Wessel and Smith, 1998; www.soest.hawaii.edu/gmt, last accessed December 2017). 

ACKNOWLEDGMENTS

This study was conducted during the appointment of the first author at the Pacific Earthquake Engineering Research Center (PEER) at the University of California, Berkeley. The authors thank the National Research Institute for Earth Science and Disaster Resilience (NIED), the Institute of Earth Sciences (IES), and the Global Centroid Moment Tensor (CMT) Project for granting access to their seismic moment estimates. The authors appreciate the comments provided by Liang of the IES on the history of the computational methodology used to estimate the seismic moment by the Broadband Array in Taiwan for Seismology. The authors also appreciate the comments by Nicholas Kuehn regarding the uncertainties in moment magnitude for developing the database. The continued encouragement of Harold Magistrale of FM Global is greatly appreciated. The review comments and suggestions by three anonymous reviewers and Editor-in-Chief Zhigang Peng significantly improved the article. The opinions, findings, and conclusions or recommendations expressed in this material are those of the authors and do not necessarily reflect those of the sponsoring agencies.

REFERENCES

- Abrahamson, N. A., and W. J. Silva (2007). Abrahamson & Silva NGA ground motion relations for the geometric mean horizontal component of peak and spectral ground motion parameters, *Pacific Earthquake Engineering Research Center*, University of California, Berkeley, available at http://peer.berkeley.edu/pdf/AbraSil_2007_v2.pdf (last accessed January 2018).
- Atkinson, G. M., and S. E. McCartney (2005). A revised magnitude-recurrence relation for shallow crustal earthquakes in southwestern British Columbia: Considering the relationships between moment magnitude and regional magnitudes, *Bull. Seismol. Soc. Am.* **95**, 334–340, doi: [10.1785/0120040095](https://doi.org/10.1785/0120040095).
- Bernardi, F., J. Braunmiller, U. Kradolfer, and D. Giardini (2004). Automatic regional moment tensor inversion in the European-Mediterranean region, *Geophys. J. Int.* **157**, no. 2, 703–716.
- Chang, W.-Y., K.-P. Chen, and Y.-B. Tsai (2016). An updated and refined catalog of earthquakes in Taiwan (1900–2014) with homogenized M_w magnitudes, *Earth Planets Space* **68**, 45, doi: [10.1186/s40623-016-0414-4](https://doi.org/10.1186/s40623-016-0414-4).
- Chen, K.-C., W.-T. Liang, Y.-H. Liu, W.-G. Huang, and J.-H. Wang (2008). Seismic moments of Taiwan's earthquakes evaluated from a regional broadband array, *Earth Planets Space* **60**, 559–564.
- Chen, K.-P., and Y.-B. Tsai (2008). Short note: A catalog of Taiwan earthquakes (1900–2006) with homogenized M_w magnitudes, *Bull. Seismol. Soc. Am.* **98**, no. 1, 483–489.
- Dreger, D., and D. V. Helmberger (1993). Determination of source parameters at regional distances with single station or sparse network data, *J. Geophys. Res.* **98**, 8107–8125.
- Dziewonski, A. M., T.-A. Chou, and J. H. Woodhouse (1981). Determination of earthquake source parameters from waveform data for studies of global and regional seismicity, *J. Geophys. Res.* **86**, 2825–2852, doi: [10.1029/JB086iB04p02825](https://doi.org/10.1029/JB086iB04p02825).

- Ekström, G., M. Nettles, and A. M. Dziewonski (2012). The global CMT project 2004–2010: Centroid-moment tensors for 13,017 earthquakes, *Phys. Earth Planet. In.* **200/201**, 1–9, doi: [10.1016/j.pepi.2012.04.002](https://doi.org/10.1016/j.pepi.2012.04.002).
- Engdahl, E. R. (2006). Application of an improved algorithm to high precision relocation of ISC test events, *Phys. Earth Planet. In.* **158**, 14–18.
- Engdahl, E. R., R. van der Hilst, and R. Buland (1998). Global teleseismic earthquake relocation with improved travel times and procedures for depth determination, *Bull. Seismol. Soc. Am.* **88**, 722–743.
- EPRI/DOE/NRC (2012). Central and eastern United States seismic source characterization for nuclear facilities, *Technical Report, NUREG-2115*.
- Fukuyama, E., M. Ishida, D. S. Dreger, and H. Kawai (1998). Automated seismic moment tensor determination by using on-line broadband seismic waveforms, *Zisin* **51**, 149–156 (in Japanese with English abstract).
- Gasparini, P., B. Lolli, G. Vannucci, and E. Boschi (2012). A comparison of moment magnitude estimates for the European–Mediterranean and Italian regions, *Geophys. J. Int.* **190**, 1733–1745, doi: [10.1111/j.1365-246X.2012.05575.x](https://doi.org/10.1111/j.1365-246X.2012.05575.x).
- Gehl, P., L. F. Bonilla, and J. Douglas (2011). Accounting for site characterization uncertainties when developing ground-motion prediction equations, *Bull. Seismol. Soc. Am.* **101**, no. 3, 1101–1108, doi: [10.1785/0120100246](https://doi.org/10.1785/0120100246).
- Hanks, T. C., and H. Kanamori (1979). A moment magnitude scale, *J. Geophys. Res.* **84**, 2348–2350.
- Hsu, Y.-J., M. Ando, S.-B. Yu, and M. Simons (2012). The potential for a great earthquake along the southernmost Ryukyu subduction zone, *Geophys. Res. Lett.* **39**, L14302, doi: [10.1029/2012GL052764](https://doi.org/10.1029/2012GL052764).
- Huang, P. (2017). Crustal seismic stress field in Taiwan inferred from regional-scale damped inversion of AutoBATS CMT solutions, *Master Thesis*, Institute of Applied Geosciences, National Taiwan Ocean University.
- Institute of Earth Sciences (IES) (1996). *Broadband Array in Taiwan for Seismology*, Institute of Earth Sciences, Academia Sinica, Taiwan, Other/Seismic Network, doi: [10.7914/SN/TW](https://doi.org/10.7914/SN/TW).
- Johnson, R. A., and D. W. Wichern (2002). *Applied Multivariate Statistical Analysis*, Fifth Ed., Prentice Hall, Inc., Upper Saddle River, New Jersey, 461 pp.
- Kagan, Y. Y. (2002). Modern California earthquake catalogs and their comparison, *Seismol. Res. Lett.* **73**, no. 6, 921–929.
- Kao, H., P. R. Jian, K. F. Ma, B. S. Huang, and C. C. Liu (1998). Moment-tensor inversion for offshore earthquakes east of Taiwan and their implications to regional collision, *Geophys. Res. Lett.* **25**, 3619–3622.
- Kishida, T., S. Derakhshan, S. Muin, R. B. Darragh, Y. Bozorgnia, N. Kuehn, and D. Y. Kwak (2018). Multivariate predictions of moment magnitude for small-to-moderate magnitude earthquakes in Iran, *Earthq. Spectra* doi: [10.1193/050917EQS086M](https://doi.org/10.1193/050917EQS086M) (in press).
- Konstantinou, K. I. (2015). Moment magnitude estimates for earthquakes in the Greek region: A comprehensive comparison, *Bull. Seismol. Soc. Am.* **105**, no. 5, 2555–2562, doi: [10.1785/0120150088](https://doi.org/10.1785/0120150088).
- Kubo, A., E. Fukuyama, H. Kawai, and K. Nonomura (2002). NIED seismic moment tensor catalogue for regional earthquakes around Japan: Quality test and application, *Tectonophysics* **356**, 23–48.
- Kuehn, N. M., and N. A. Abrahamson (2018). The effect of uncertainty in predictor variables on the estimation of ground-motion prediction equations, *Bull. Seismol. Soc. Am.* **108**, no. 1, 358–370, doi: [10.1785/0120170166](https://doi.org/10.1785/0120170166).
- Lee, S.-J., W.-T. Liang, H.-W. Cheng, F.-S. Tu, K.-F. Ma, H. Tsuruoka, H. Kawakatsu, B.-S. Huang, and C.-C. Liu (2014). Towards real-time regional earthquake simulation. I: Real-time moment tensor monitoring (RMT) for regional events in Taiwan, *Geophys. J. Int.* **196**, no. 1, 432–446, doi: [10.1093/gji/ggt371](https://doi.org/10.1093/gji/ggt371).
- Nakamura, M. (2009). Fault model of the 1771 Yaeyama earthquake along the Ryukyu trench estimated from the devastating tsunami, *Geophys. Res. Lett.* **36**, L19307, doi: [10.1029/2009GL039730](https://doi.org/10.1029/2009GL039730).
- Papazachos, B. C., A. A. Kiratzi, and B. G. Karacostas (1997). Toward a homogeneous moment-magnitude determination for earthquakes in Greece and the surrounding area, *Bull. Seismol. Soc. Am.* **87**, no. 2, 474–483.
- Rhoades, D. A. (1997). Estimation of attenuation relations for strong-motion data allowing for individual earthquake magnitude uncertainties, *Bull. Seismol. Soc. Am.* **87**, no. 6, 1674–1678.
- Scherbaum, F., F. Cotton, and P. Smit (2004). On the use of response spectral-reference data for the selection and ranking of ground-motion models for seismic-hazard analysis in regions of moderate seismicity: The case of rock motion, *Bull. Seismol. Soc. Am.* **94**, no. 6, 2164–2185.
- Stafford, P. J. (2014). Crossed and nested mixed-effects approaches for enhanced model development and removal of the ergodic assumption in empirical ground-motion models, *Bull. Seismol. Soc. Am.* **104**, no. 2, 702–719, doi: [10.1785/0120130145](https://doi.org/10.1785/0120130145).
- Thio, H. K., and H. Kanamori (1995). Moment-tensor inversions for local earthquakes using surface waves recorded at TERRAscope, *Bull. Seismol. Soc. Am.* **85**, no. 4, 1021–1038.
- Wessel, P., and W. H. F. Smith (1998). New, improved version of the generic mapping tools released, *Eos Trans. AGU* **79**, 579.

*Tadahiro Kishida*¹

*Civil Infrastructure and Environmental Engineering
Khalifa University of Science and Technology
Abu Dhabi, P.O. Box 127788
United Arab Emirates
tadahiro.kishida@kustar.ac.ae*

*Robert B. Darragh
Pacific Engineering and Analysis
856 Sea View Drive
El Cerrito, California 94530 U.S.A.
bbalindavis@gmail.com*

*Yousef Bozorgnia
Department of Civil and Environmental Engineering
University of California
Los Angeles, California 90095 U.S.A.
Yousef.bozorgnia@UCLA.edu*

*Chun-Hsiang Kuo
National Center for Research on Earthquake Engineering
200, Section 3, HsinHai Road
Taipei 10668, Taiwan
chkuo@ncree.narl.org.tw*

*Hongjun Si
Earthquake Research Institute
The University of Tokyo
1-1-1 Yayoi, Bunkyo-ku
Tokyo 113-0032, Japan
shj@eri.u-tokyo.ac.jp*

Published Online 21 March 2018

¹ Previously at University of California, Berkeley, California 94720 U.S.A.